The Role of Enzyme Isomerization in the Native Catalytic Cycle of the ATP Sulfurylase−GTPase System†

Jiang Wei, Changxian Liu, and Thomas S. Leyh*

Department of Biochemistry, Albert Einstein College of Medicine, 1300 Morris Park Avenue, Bronx, New York 10461-1926

Received September 22, 1999; Revised Manuscript Received February 4, 2000

ABSTRACT: ATP sulfurylase, from *E. coli* K-12, is a GTPase•target complex that conformationally couples the free energies of GTP hydrolysis and activated sulfate (adenosine 5′-phosphosulfate, or APS) synthesis. Energy coupling is achieved by an allosterically driven isomerization that switches on and off chemistry at specific points in the catalytic cycle. This coupling mechanism is derived from the results of model studies using analogue complexes that mimic different stages of the native catalytic cycle. The current investigation extends the analogue studies to the native catalytic cycle. Isomerization is monitored using the fluorescent, guanine nucleotide analogues mGMPPNP (3′-*O*-(*N*-methylanthraniloyl)-2′-deoxyguanosine 5′-[β,γ-imido]triphosphate) and mGTP [3′-*O*-(*N*-methylanthraniloyl)-2′-deoxyguanosine 5′-triphosphate]. The isomerization is shown to be initiated by an allosteric interaction that requires the simultaneous occupancy of all three substrate-binding sites. Stopped-flow fluorescence and single-turnover studies were used to define and quantitate the isomerization mechanism, and to show that the isomerization precedes and rate-limits both GTP hydrolysis and APS synthesis. These findings are incorporated into a model of the energy-coupling mechanism.

The metabolic assimilation of sulfate, a nonreactive compound, requires that it be chemically activated. In *E. coli* and other gram-negative bacteria, activated sulfate (adenosine 5′-phosphosulfate, or APS)[1] is reduced to hydrogen sulfide, and subsequently incorporated into reduced sulfur metabolites (*1*). Anaerobes can use sulfate reduction as a source of electrons for their electron-transport chains (*2, 3*). Mammals use activated sulfate for an entirely different purpose: sulfuryl group ($-SO_3^-$) transfer. This transfer reaction regulates the activities of a diverse group of metabolites including steroid (*4*−*8*) and peptide hormones (*9, 10*), neurotransmitters (*11*), and carbohydrate recognition elements (*12, 13*).

The activation of sulfate is achieved by transferring the adenylyl moiety (AMP∼) from ATP to sulfate (reaction 1):

$$ATP^{4-} + SO_4^{2-} \rightleftarrows APS^{2-} + P_2O_7^{4-} \qquad (1)$$

The Gibbs potential of the phosphoric−sulfuric acid anhydride bond is extremely large [$\Delta G^{0'}_{\text{hydrolysis}} = -19$ kcal/mol (*14*−*16*)]. Thus, despite the fact that APS synthesis is coupled to cleavage of the ATP α,β-bond (*17*), the equilibrium constant for APS formation is remarkably unfavorable [1.1×10^{-8}, pH 8.0 (*15, 16*)]. This formidable energetic barrier is overcome in *E. coli* (*18*), and other gram-negative bacteria (*19*), by coupling the free energies of GTP hydrolysis (reaction 2) and APS synthesis (*20, 21*):

$$GTP^{4-} + H_2O \rightleftarrows GDP^{3-} + HPO_4^{2-} + H^+ \qquad (2)$$

These two reactions are catalyzed and energetically linked by the enzyme ATP sulfurylase (ATP:sulfate adenylyltransferase, EC 2.7.7.4) from *E. coli*. This enzyme is a tetramer of heterodimers. Each heterodimer is composed of a CysD (35 kDa) and a CysN (53 kDa) subunit, which catalyze APS synthesis and GTP hydrolysis, respectively (*18, 22*). ATP sulfurylase is a rare example of a GTPase•target complex in which structural changes in the catalytic cycle couple the free energy of GTP hydrolysis (reaction 2) to a second, small-molecule reaction (*20, 21*).

The catalytic cycle of ATP sulfurylase includes an isomerization that is concomitant with a large increase in both the affinity and reactivity of GTP (*23, 24*). The isomerization is, in effect, a molecular switch that controls the GTPase activity of the enzyme. Defining where and how this switch is thrown is the focus of this study. Certain GTPase activators, which form complexes at the APS active site that mimic discrete stages of the catalytic cycle, can elicit the isomerization; others cannot. The activator-complex dependence of the isomerization suggests that it occurs at a specific stage of the APS-forming reaction, and implies an interdependence of these chemistries that is capable of coupling their free energies. The strength and weakness of the activator approach is that the individual complexes provide "snapshots" of the enzyme's behavior at a particular

† Supported by National Institutes of Health Grant GM54469.

* Correspondence should be addressed to this author at the Department of Biochemistry, Albert Einstein College of Medicine, 1300 Morris Park Ave., Bronx, NY 10461-1926. Phone: 718-430-2857. Fax: 718-430-8565. E-mail: leyh@aecom.yu.edu.

[1] Abbreviations: APS, adenosine 5′-phosphosulfate; EDTA, ethylenediamine-*N*,*N*,*N*′,*N*′-tetraacetic acid; mGMPPNP, 3′-*O*-(*N*-methylanthraniloyl)-2′-deoxyguanosine 5′-[β,γ-imido]triphosphate; Hepes, 4-(2-hydroxyethyl)-1-piperazineethanesulfonic acid; PEI-F, poly(ethylenimine)−cellulose-F; Tris, tris(hydroxymethyl)aminomethane; U (unit(s)), micromoles of substrate converted to product per minute at V_{max}.

10.1021/bi992210y CCC: $19.00
Published on Web 03/23/2000

stage of its catalytic cycle (*25, 26*). The behavior between these "points" must be inferred. The current study extends the activator complex studies to the native catalytic cycle.

MATERIALS AND METHODS

Inorganic pyrophosphatase (yeast), NADH, PEP, AMP, ATP, GTP, SO_4, EDTA, Hepes, Tris, and $MgCl_2$ were purchased from the Sigma Chemical Co. Pyruvate kinase (rabbit muscle), lactate deyhdrogenase (rabbit muscle), and GMPNP were purchased from Boehringer Mannheim. Poly(ethylenimine)−cellulose-F thin-layer chromatography (PEI-F TLC) plates were obtained from EM Science. Radiochemicals were purchased from NEN DuPont Corp. The synthesis and purification of the fluorescent guanine nucleotide analogues mGMPPNP and mGTP have been described elsewhere (*23*).

Purification of ATP Sulfurylase. The native *E. coli* ATP sulfurylase used in these studies is purified from an *E. coli* K-12 strain containing an expression plasmid that produces the enzyme at high levels (*18, 23*). The specific activity of the ATP sulfurylase, assayed according to a published protocol (*18*), was 0.74 U/mg.

Stopped-Flow Fluorescence Measurements. Measurements were made using a Photophysics (model SX-17MV) instrument. The samples were equilibrated and experiments performed at 25 (±2) °C. The samples were excited with 350 nm light; light emitted above 400 nm was detected. Typically, a 300 V photomultiplier gain was used with a variable bias offset. The signal was acquired without filtering; five to seven scans were averaged. The sequential mixing experiments were performed using an SX-17MV instrument with an SQ1 sequential-mixing accessory. The data were fit, and the experimental uncertainties were obtained using the Photophysics data analysis software, which employs a Marquardt−Levenberg fitting algorithm. The concentration dependence of reaction rates was evaluated by varying the enzyme, rather than ligand, concentration (*24*). This strategy has been described previously (*27*).

Effects of SO_4 on GTP Hydrolysis (the Initial-Rate Assay). GTP hydrolysis was monitored continuously at 340 nm by coupling the production of GDP to the oxidation of NADH using the coupling enzymes pyruvate kinase and lactate dehydrogenase. The assay conditions were as follows: ATP sulfurylase (32 nM), pyruvate kinase (5.4 U/mL), lactate dehydrogenase (3.9 U/mL), NADH (0.10 mM), $MgCl_2$ ([GTP] + 1.0 mM), Hepes/K^+ (50 mM, pH 8.0), $T = 25$ (±2) °C. The initial velocities were determined in duplicate at each of the 16 conditions obtained using a 4 × 4 matrix of GTP and SO_4 concentrations. The concentrations were the following: GTP, 0.830, 0.092, 0.049, 0.033 mM; SO_4, 8.0, 2.0, 1.1, 0.80 mM. The rates were determined during the first 5−10% of the reaction. The coupling enzymes were desalted into the buffer used for the initial-rate assays; their specific activities were measured in that same buffer (*28, 29*) [pyruvate kinase activity was determined using GDP as the substrate (*30*)]. The coupling enzyme concentrations used in the initial-rate assays were sufficient to achieve the steady-state within 4 s (*31*). The data were fit using the weighted least-squares program *Sequeno*, developed by Cleland (*32*).

The assay conditions used in the sulfate inhibition study were the same as those described above. The GTP concentration was held fixed and saturating at 0.51 mM ($12K_m$). The SO_4 concentration was varied (see text), and the data were fit using eq 1, which is derived from a general inhibition mechanism:

$$v = \frac{k_{cat}[SO_4]}{K_{a(SO_4)} + [SO_4] + [SO_4]^2/K_{i(app)}} \quad (3)$$

in which ligand binding is at equilibrium, there is one inhibitor binding site per active site, and inhibitor binding completely prevents turnover (*33*). K_a and $K_{i(app)}$ are the steady-state dissociation constants for the binding of SO_4 to the E·GTP and E·GTP·SO_4 complexes. k_{cat} and K_a were obtained from the initial-rate study described in the preceding paragraph (see Results and Discussion). The data were fit using the program *Sigma Plot*, which uses the Marquardt−Levenberg fitting algorithm. The value of $K_{i(app)}$ obtained from the fit is 33 (±3) mM.

Pre-Steady-State Studies Using Radiolabeled Substrates. The protocols for the ATP hydrolysis and APS synthesis studies were performed in a similar manner. The reactions were initiated by the addition of ATP sulfurylase, and quenched by addition of a 0.10 M stock of EDTA, pH 9.5, to a final concentration of 50 mM. Immediately following the quench, the enzyme was inactivated by heating the reaction solutions in a boiling water bath for 1.0 min. The solutions were then spotted onto PEI-F TLC plates, and the radiolabeled reactants were separated using a 0.90 M LiCl mobile phase (*34*). The reactants were quantitated using the AMBIS two-dimensional radioactivity detector (*35*). Two time points were taken at each of five different time intervals. Progress curves were constructed and fit by least squares to obtain k_{cat}.

RESULTS AND DISCUSSION

The E·ATP and E·SO_4 Complexes. Stopped-flow fluorescence experiments were performed to assess whether mGMPPNP binding to the E·ATP and E·SO_4 complexes occurs in two phases, indicative of an isomerization. The binding of mGMPPNP to the E·ATP complex is shown in panel A of Figure 1. The solid line passing through the data is the behavior predicted by a best-fit, single-step binding model; the residual plot is shown in panel B. The data are fit well by the single-step model (see residual plot, panel B, Figure 1). The absence of a second phase in the binding reaction indicates either that the enzyme does not isomerize or that the fluorescence change associated with the isomerization is too small to detect. It is possible that the interactions between mGMPPNP and the enzyme are essentially unaffected by the interactions of ATP with its binding site. Alternatively, perhaps these nucleotides do interact, but the resulting change in the environment of the fluorescent moiety of mGMPPNP does not cause a detectable change in fluorescence—this is the case with AMP binding (*24*). A more general test for ATP/GTP interactions is to assess whether the binding of ATP alters the rate constants governing the binding of mGMPPNP. These constants were obtained from a study of the [E·ATP] dependence of k_{obs} for mGMPPNP binding (panel C, Figure 1). The results are $k_{on} = 4.9\ (\pm 0.5) \times 10^5\ M^{-1}\ s^{-1}$, $k_{off} = 13\ (\pm 0.1)\ s^{-1}$, and $K_d = 27\ \mu M$. These constants are remarkably similar to those

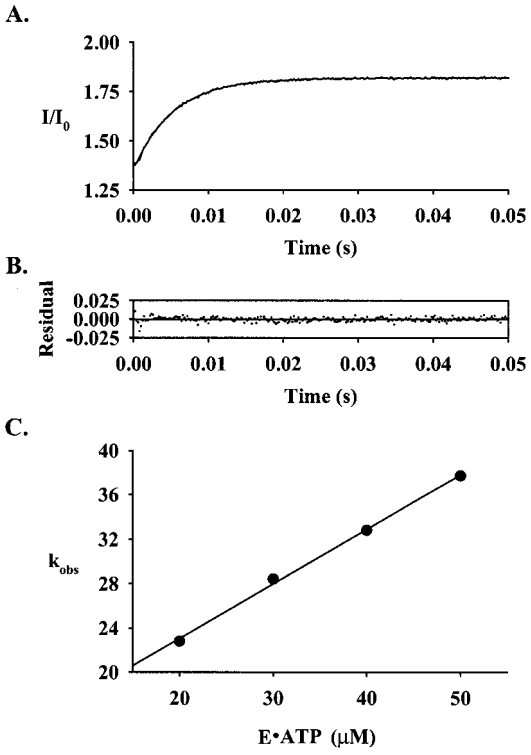

FIGURE 1: Binding of mGMPPNP to the E·ATP complex of ATP sulfurylase. The reaction was followed by monitoring by the change in fluorescence of the mGMPPNP that occurs as it binds to the enzyme. Panel A: A binding reaction progress curve. The reaction was initiated by mixing a solution containing ATP sulfurylase (40 μM), ATP (0.5 mM), Mg^{2+} (1.5 mM), and Tris/HCl (50 mM, pH 8.0) with an equal volume of an identical solution that did not contain enzyme, but did contain mGMPPNP (4.0 μM). The smooth curve passing through the data represents the best-fit of a single-exponential model. The solutions were equilibrated, and the experiments were performed at $T = 25$ ($\pm$2) °C. Panel B: The *residual plot*, the difference between the actual and best-fit values shown in panel A. Panel C: The concentration dependence of k_{obs} for mGMPPNP binding to the E·ATP complex of ATP sulfurylase. The experimental conditions were identical to those described above except that the E·ATP concentration was varied as indicated. k_{obs} at each concentration was obtained by fitting the progress curves to a single-exponential model.

previously determined for the binding of mGMPPNP to the nonisomerized form of the enzyme [$k_{on} = 2.9 \times 10^5$ M^{-1} s^{-1}, $k_{off} = 7.9$ s^{-1}, $K_d = 27$ μM (*23*)]. Thus, the contacts formed upon the binding of ATP do not significantly influence the environment of mGMPPNP (isomerization does not occur).

The mGMPPNP·E·AMP·PP_i complex mimics an intermediate stage of the catalytic cycle in which the α,β-bond of ATP has been cleaved (*23*). This complex isomerizes, and the isomerization reaction is quite favorable, $K_{iso} = 3000$. The mGMPPNP·E·ATP complex occurs at an early stage of the catalytic cycle, and does not isomerize. Thus, it appears that the very favorable energetics of the isomerization provide a driving force for α,β-bond cleavage.

ATP sulfurylase slowly hydrolyzes the α,β-bond of ATP in a reaction that requires GTP hydrolysis (*36*). The rate experiments described above involve mixing a solution containing ATP sulfurylase, ATP, and Mg^{2+} [the (+)-enzyme solution] with a concentration-matched solution that lacks enzyme, and contains mGMPPNP (see the Figure 1 legend). Given the high enzyme concentration of the (+)-enzyme solution ($\leq$40 μM), it seemed prudent to determine whether significant hydrolysis occurred prior to mixing. Hydrolysis was measured (see Materials and Methods) using [α-^{32}P]-ATP under conditions comparable to those of the (+)-enzyme solution [ATP sulfurylase (50 μM), ATP (1.0 mM, 0.5 μCi/μL), Mg^{2+} (2.0 mM), Tris/HCl (50 mM, pH 8.0), $T = 25$ ($\pm$2) °C]. No cleavage was detected over 25 min. It was also important to test the extent to which cleavage occurs in the mGPMPNP·E·ATP complex that forms during the binding reaction. Cleavage was again measured using [α-^{32}P]-ATP; the conditions were as follows: ATP sulfurylase (50 μM), ATP (1.0 mM, 0.5 μCi/μL), GMPPNP (0.50 mM, 19 $\times$ K_d), Mg^{2+}(2.5 mM), inorganic pyrophosphatase [1.0 U/mL, added to prevent inhibition by PP_i (*23*)], Tris/HCl (50 mM, pH 8.0), $T = 25$ ($\pm$2) °C. Cleavage did occur, but was extremely slow [$k_{cat} = 0.05$ ($\pm$0.01) min^{-1}]. During the $\sim$50 ms required for the binding reaction, <0.25% of the ATP in the mGPMPNP·E·ATP complex is hydrolyzed. These controls establish that the binding experiments report on binding exclusively to the substrate (i.e, E·ATP) forms of the enzyme.

Designing experiments to test the effects of sulfate on the enzyme isomerization requires the affinity constants for the binding of sulfate to E and E·GTP. Sulfate is a modest activator of GTP hydrolysis, and it was therefore possible to assess its affinity by intial-rate methods. Previous isotope trapping experiments indicate that ligand binding is at, or near, equilibrium during turnover; hence, the kinetic constants for the activation should be excellent approximations of thermodynamic binding constants. The intitial rate study used a 4 $\times$ 4 matrix of GTP and SO_4 concentrations (see Materials and Methods). The data (not shown) were fit using the *Sequeno* program developed by Cleland (*32*). The results were as follows: $K_{a(SO_4)} = 14$ ($\pm$1) mM, $K_{m(GTP)} = 45$ ($\pm$9) μM, $K_{i(SO_4)} = 15$ ($\pm$3) mM, $K_{i(GTP)} = 48$ ($\pm$5) mM, and $k_{cat} = 8.8$ min^{-1} (i.e., a 2.5-fold increase over the nonactivated rate). $K_{a(SO_4)}$ and $K_{i(SO_4)}$, the dissociation constants for the GTP·E·SO_4 and E·SO_4 complexes, respectively, are quite high. At concentrations >10 mM, SO_4 begins to significantly inhibit the GTPase activity of ATP sulfurylase (see panel A, Figure 2). At 10 mM SO_4, $\sim$31% of the enzyme has SO_4 bound at the GTPase activating site. The binding of mGMPPNP to ATP sulfurylase at 10 mM SO_4 shows no sign of a second phase (panel B, Figure 2). At higher concentrations of SO_4, binding is still monophasic; however, the overall change in fluorescence intensity decreases. Thus, it appears that, like ATP, the effects of SO_4 on the isomerization, if any, fall below the limits of detection.

The Michaelis (E·ATP·SO_4) Complex. ATP sulfurylase catalyzes APS synthesis slowly in the absence of GTP; hence, the E·ATP·SO_4 complex represents one of several Michaelis, or reactive, complexes that this enzyme can form. A progress curve for the binding of mGMPPNP to the E·ATP·SO_4 complex is shown in panel A of Figure 3. The curve demonstrates at least two well-separated phases, indicative of an isomerization. This is corroborated by the residual plots (panels B) which depict the difference between the actual data and the progress curves simulated using the best-fit parameters obtained from the one- and two-step models. The residual obtained using the one-step model shows considerable deviation from zero, indicating that the model is inadequate to describe the system's behavior. The two-step

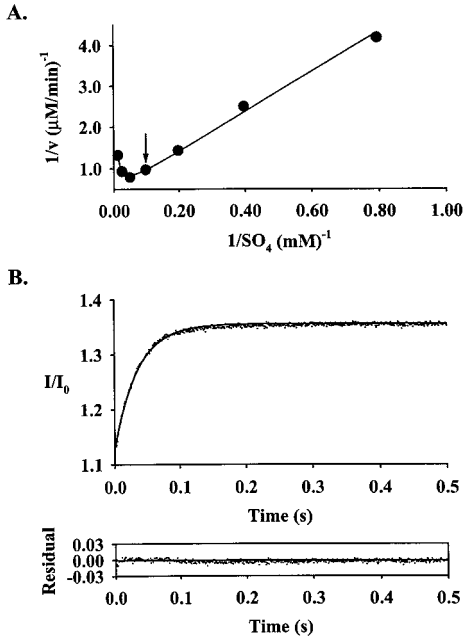

FIGURE 2: Binding of mGMPPNP to the E·SO_4 complex of ATP sulfurylase. Panel A: The effects of SO_4 on the initial rate of GTP hydrolysis. The initial rate of GTP hydrolysis is shown as a function of SO_4 concentration. The experimental conditions are outlined in the initial-rate section of Materials and Methods. The activation of GTP hydrolysis is linear with SO_4 concentration as high as 10 mM (indicated by the arrow); inhibition is observed above this concentration. The solid line represents the data predicted by the best-fit of eq 3. Panel B: The binding of mGMPPNP to the E·SO_4 complex of ATP sulfurylase at 10 mM SO_4. Binding was monitored by following the change in fluorescence intensity of mGMPPNP as it binds to the enzyme. The reaction was initiated by mixing a solution containing ATP sulfurylase (40 μM), SO_4 (1.0 mM), Mg^{2+} (2.0 mM), and Tris/HCl (50 mM, pH 8.0) with an equal volume of an identical solution that did not contain enzyme, but did contain mGMPPNP (4.0 μM). The smooth curve passing through the data represents the best-fit of a single-exponential model. The solutions were preequilibrated, and the experiments were performed at $T =$ 25 (±2) °C.

model, however, provides an excellent fit, indicating two or more steps in the binding reaction.

To further confirm the biphasic nature of the binding reaction, and to begin to obtain the rate constants that govern it, the observed rate constants for the first [$k_{1(obs)}$] and second phases [$k_{2(obs)}$] of the reaction were studied as a function of the concentration of the Michaelis complex, E·ATP·SO_4. $k_{1(obs)}$ and $k_{2(obs)}$ are given by eqs 4 and 5, respectively (*37*, *38*).

$$k_{1(obs)} = k_1[E] + k_{-1} + k_2 + k_{-2} \quad (4)$$

$$k_{2(obs)} = \frac{k_1[E](k_2 + k_{-2}) + k_{-1}k_{-2}}{k_1[E] + k_{-1} + k_2 + k_{-2}} \quad (5)$$

Equation 4 describes a straight line, with slope k_1 and intercept $k_{-1} + k_2 + k_{-2}$. Equation 5 describes a rectangular hyperbola that plateaus at $k_{2(obs)} = k_2 + k_{-2}$. The excellent fit of eqs 4 and 5 to the experimentally determined concentration dependence of $k_{1(obs)}$ and $k_{2(obs)}$ (panel C, Figure 3) provides strong support for the two-step model. Subtracting the plateau value of $k_{2(obs)}$ from the $k_{1(obs)}$ intercept yields k_{-1}, which, along with k_1, can be used to calculate the equilibrium constant for the first step in the binding reaction.

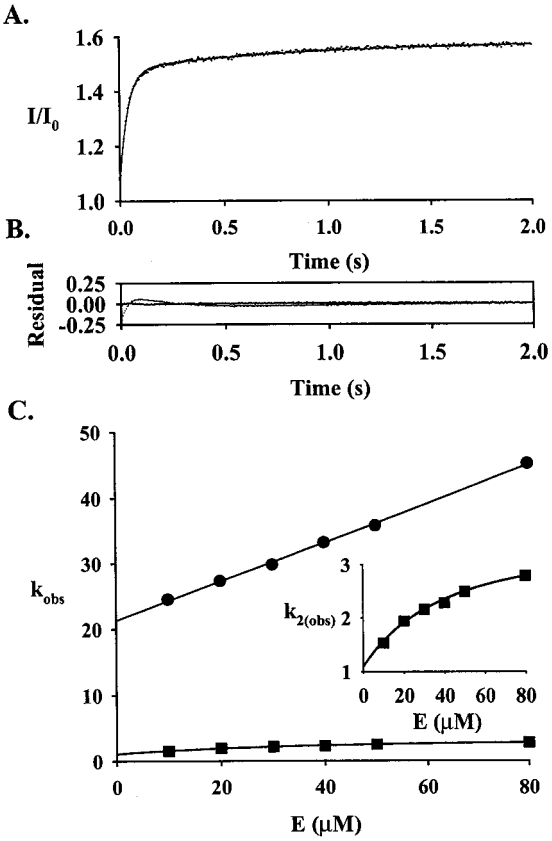

FIGURE 3: Binding of mGMPPNP to the Michaelis (E·ATP·SO_4) complex of ATP sulfurylase. The reaction was followed by monitoring the change in fluorescent intensity of mGMPPNP as it binds to the E·ATP·SO_4 complex. Panel A: The binding of mGMPPNP to the E·ATP·SO_4 complex. The reaction was initiated by mixing a solution containing ATP sulfurylase (40 μM), ATP (0.5 mM), SO_4 (1.0 mM), $MgCl_2$ (2.5 mM), and Tris/HCl (50 mM, pH 8.0) with an equal volume of a concentration-matched solution that did not contain ATP sulfurylase, but did contain mGMPPNP (4.0 μM). The solutions were thermally equilibrated at 25 (±2) °C. The smooth curve passing through the data is the intensity change predicted by the two-step binding model. Panel B: The residual plots obtained using one- and two-step binding models. The one-step model resulted in significant deviation from zero. Panel C: The concentration dependence of the observed rate constants for the binding of mGMPPNP. The experiments were performed as described for panel A of this legend except that the enzyme concentration was varied as indicated. The data were fit using a two-step binding model; $k_{1(obs)}$ and $k_{2(obs)}$ are represented by the circles (●) and squares (■), respectively. The *y*-axis is expanded in the inset to provide better visualization of the $k_{2(obs)}$ data.

k_1, k_{-1}, and K_d are 0.34 (±0.02) × 10^6 M^{-1} s^{-1}, 17 (±1) s^{-1}, and 50 μM, respectively.

To test whether the isomerization precedes and rate-limits GTP hydrolysis, the binding and hydrolysis of mGTP by the E·ATP·SO_4 complex were studied under conditions identical (except for the substitution of mGTP for mGMPPNP) to those described for the mGMPPNP binding experiment associated with panel A of Figure 3. If the observed rate constants for the isomerization of the mGMPPNP·E·ATP·SO_4 complex are the same as those for cleavage of the β,γ-bond of mGTP, the isomerization precedes and rate-limits hydrolysis. β,γ-bond cleavage causes the fluorescent intensity of the enzyme-bound nucleotide to decrease (*23*). The stopped-flow fluorescence profile of the mGTP binding and hydrolysis reaction is clearly biphasic (Figure 4). The

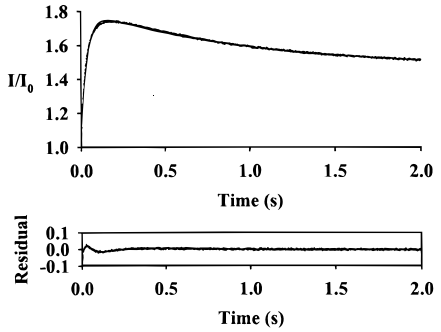

FIGURE 4: Binding and hydrolysis of mGTP by the Michaelis (E·ATP·SO_4) complex of ATP sulfurylase. The reactions were followed by monitoring the changes in fluorescent intensity that mGTP undergoes as it binds to, and is hydrolyzed by, the enzyme. For purposes of direct comparison, the conditions of this study were identical to those described in panel A of Figure 3, except for the substitution of mGTP for mGMPPNP.

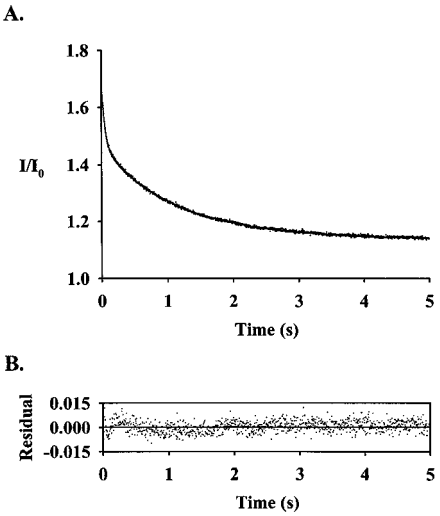

FIGURE 5: Release of mGMPPNP from the mGMPPNP·E·ATP·SO_4 complex of ATP sulfurylase. The release reaction was monitored by following the mGMPPNP fluorescence intensity changes that occur at each step of the reaction. The first stage of the reaction (assembling the mGMPPNP·E·ATP·SO_4 complex) was initiated by mixing a solution containing ATP sulfurylase (80 μM), mGMPPNP (8.0 μM), ATP (0.50 mM), SO_4 (1.0 mM), $MgCl_2$ (2.5 mM), and Tris/HCl (50 mM, pH 8.0), $T = 25$ ($\pm$2) °C, with an equal volume of a solution that was identical except that it contained no enzyme and mGMPPNP, at 8.0 μM. The mixture was then "aged" during a 5.0 s delay time in which the mGMPPNP·E·ATP·SO_4 complex assembles. At the end of the delay, the irreversible release of mGMPPNP is initiated by mixing with an equal volume of a solution containing GMPPNP (a nonfluorescent competitive ligand, 0.40 mM), ATP (0.50 mM), SO_4 (1.0 mM), $MgCl_2$ (2.9 mM), Tris/HCl (50 mM, pH 8.0), $T = 25$ ($\pm$2) °C. The residual plot was obtained using a two-step release model.

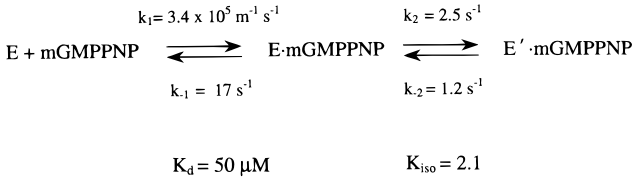

FIGURE 6: Quantitated two-step isomerization model. E represents the E·ATP·SO_4 complex; E′ indicates the isomerized form of this complex.

increasing intensity associated with the first phase is due to the binding of mGTP; the decreasing second phase is due to hydrolysis of the β,γ-bond (*23*). The observed rate constants for binding and hydrolysis of mGTP [28 ($\pm$1) and 1.9 ($\pm$0.1) s^{-1}, respectively] are extremely simliar to those for the binding and isomerizaton reactions involving mGMPPNP [27 ($\pm$1) and 1.9 ($\pm$0.1) s^{-1}, respectively]. Thus, as is the case for the isomerization observed with the mGMPPNP·E·AMP·PP_i complex, the isomerization associated with the mGMPPNP·E·ATP·SO_4 complex precedes and rate-limits GTP hydrolysis.

While the data shown in Figure 3 clearly demonstrate two steps in the binding reaction, they do not address the important mechanistic issue of whether the isomerization occurs before or after the binding of mGMPPNP. In favorable cases, this can be resolved by monitoring the behavior of the system as the nucleotide is released from the enzyme (*24*). If the isomerization occurs prior to ligand binding, a single enzyme·ligand complex is formed, and the release reaction is monophasic. If the ligand adds prior to the isomerization (i.e., the isomerization is driven by the binding of mGMPPNP), two enzyme·ligand complexes form, and it is possible to observe two phases in the release reaction.

The release experiment was performed using a sequential mixing strategy in which the formation of the mGMPPNP·E·ATP·SO_4 complex is initiated by rapidly mixing two solutions, neither of which hydrolyzes the α,β-bond of ATP at a significant rate. The complex forms in the fixed-variable time interval (the delay time) immediately following the first mix. The release of mGMPPNP is initiated at the end of the delay interval by rapid-mixing with a solution containing the nonfluorescent, competitive ligand, GMPPNP, in large excess over mGMPPNP. The delay time was varied to ensure that it was long enough to allow the formation of mGMPPNP·E·ATP·SO_4 to come to completion. The final concentration of mGMPPNP is sufficient to drive >98% of the mGMPPNP into solution. Under these conditions, the release of mGMPPNP is essentially irreversible. The release reaction is clearly biphasic (Figure 5), establishing that the isomerization is indeed driven by the binding of the nucleotide.

The observed rate constants associated with the release of mGMPPNP were used to obtain k_2 and k_{-2}. $k_{1(obs)}$ and $k_{2(obs)}$ for the phases of the release reaction are obtained from eqs 4 and 5 by setting [E] (the concentration of enzyme to which mGMPPNP can bind) to zero. This simplification causes $k_{1(obs)}$ (18 s^{-1}) to equal $k_{-1}k_2/(k_{-1} + k_2 + k_{-2})$. The denominator ($k_{-1} + k_2 + k_{-2}$) is given by the intercept of eq 4. Given k_{-1} (see above), k_2 and k_{-2} can be calculated. The resulting, quantitated two-step model is shown in Figure 6.

Accurate interpretation of the ligand release experiments requires a clear description of the mGMPPNP-containing complex(es) that form during the delay interval. If ATP α,β-bond cleavage occurs during the measurement, the product complexes must be taken into account in the interpretation. Cleavage can be caused by the attack of SO_4, H_2O, or the enzyme at P_α. In the absence of SO_4, ATP sulfurylase catalyzes a GTP-dependent hydrolysis of the α,β-bond of ATP. SO_4 competes with water for the α-phosphorus, and at a saturating concentration of SO_4 ($K_d = 42$ μM), AMP synthesis is suppressed to near zero (*36*). Single-turnover experiments using [^{35}S]SO_4 have shown that the rate of APS formation from the GMPPNP·E·ATP·SO_4 complex is extremely slow [<0.08% of an active-site equiv of APS formed/min (*36*)]. Thus, APS formation is negligible during the ~5 s required for the sequential mixing experiment.

To determine whether enzyme-bound or solution-phase AMP forms during the delay interval of the sequential mixing experiment, single-turnover experiments were performed using [α-^{32}P]ATP. The conditions of these experiments were similar to those used in the delay phase of the release experiment, except that mGMPPNP was replaced by GMPPNP, at a saturating concentration. The conditions were the following: ATP sulfurylase (50 μM), [α-^{32}P]ATP (0.5 mM, SA = 0.5 μCi/μL), GMPPNP (0.5 mM), SO_4 (1.0 mM), Tris/HCl (50 mM, pH 8.0), T = 25 (±2) °C. The observed rate of ATP hydrolysis was 6% of an active-site equiv of AMP formed/min. Hence, ~0.5% of an active-site equiv of ATP will be hydrolyzed in the delay interval. At this low level, the fluorescence intensity of the mGMPPNP·E·AMP·PP_i complex [which has been characterized (*23*)] will not contribute significantly to the observed results. Thus, product does not form in significant amounts during the release experiments, and they should be interpreted solely on the basis of substrate enzyme forms.

CONCLUSIONS

The isomerized form of ATP sulfurylase is not detected in any of its two-substrate complexes. Detection requires the addition of the third ligand. These facts indicate that the reorganization of the GTP-binding site, which controls its activity, is driven by an allosteric interaction among all three of the enzyme's active sites that occurs only when they are simultaneously occupied. The addition of the third ligand alters the free-energy profile of the reaction coordinate and, in so doing, stabilizes the isomerized form of the enzyme. The effects of the addition of the third ligand on the affinity of mGMPPNP are not immediate (the affinities of mGMPPNP for the E, E·ATP, and the nonisomerized E·ATP·SO_4 complexes are comparable). Thus, the primary effects of the third ligand occur downstream from its point of addition. This hysteresis is indicative of events between the binding and reorganization that mediate the communication between the two active sites. The precise nature of these events is not yet clear.

During its catalytic cycle, ATP sulfurylase sequentially passes through the mGMPPNP·E·ATP·SO_4, and mGMPPNP·E·ATP·SO_4' complexes, and then, presumably, through a bond-open form that resembles the mGMPPNP·E·AMP·PP_i' complex (the prime indicates the isomerized form of a complex). The equilibrium constants for the isomerization reaction in these complexes are ≪1, 1.5, and 3000, respectively. Thus, the enzyme moves successively, thermodynamically downward in its catalytic cycle toward the α,β-bond-opened form. The 1400-fold greater stability of the bond-open form, which provides a substantial driving force for α,β-bond cleavage, reveals that GTP binding enhances the reactivity of the ATP−P_α by selectively stabilizing the bond-open form. This stabilization depends on the γ-phosphate of GTP—it is not seen with GDP. Once the GTP β,γ-bond is broken (it is not clear whether P_i must depart), the stabilization and its concomitant effects on the reactivity of the α,β-bond of ATP vanish. Furthermore, mGMPPNP release from the bond-open form is 277-fold slower than the β,γ-bond-breaking reaction. Thus, the further the APS-forming reaction (which is moved forward by the thermodynamic benefit of the GTP γ-phosphate) proceeds into its catalytic cycle, the less likely the escape of GTP becomes. Once the α,β-bond is cleaved, escape is nearly impossible, and the system becomes committed to its forward path, which includes the hydrolysis of the GTP β,γ-bond. These reaction-stage-dependent changes in the binding and reactivity of the active sites interdigitate the chemistries which cause them to occur in a 1:1 stoichiometry, and couple their free energies.

ACKNOWLEDGMENT

We thank Professor Lizbeth Hedstrom, Department of Biochemistry, Brandeis University, for generously allowing us to perform the sequential-mixing stopped-flow fluorescence experiments in her laboratory.

REFERENCES

1. De Meio, R. M. (1975) in *Metabolic Pathways* (Greenberg, D. M., Ed.) pp 287−347, Academic Press, New York.
2. Siegel, L. M. (1975) in *Metabolic Pathways* (Greenberg, D. M., Ed.) pp 217−276, Academic Press, New York.
3. Singleton, R. J. (1993) in *The Sulfate Reducing Bacteria: Contemporary Perspectives* (Odom, J. M., and Singleton, R. J., Eds.) pp 1−20, Springer-Verlag, New York.
4. Falany, C. N., Wheeler, J., Oh, T. S., and Falany, J. L. (1994) *J. Steroid Biochem. Mol. Biol. 48*, 369−375.
5. Falany, J. L., and Falany, C. N. (1997) *Oncol. Res. 9*, 589−596.
6. Zhang, H., Varlamova, O., Vargas, F. M., Falany, C. N., Leyh, T. S., and Varmalova, O. (1998) *J. Biol. Chem. 273*, 10888−10892.
7. Pasqualini, J. R., Schatz, B., Varin, C., and Nguyen, B. L. (1992) *J. Steroid Biochem. Mol. Biol. 41*, 323−329.
8. Kotov, A., Falany, J. L., Wang, J., and Falany, C. N. (1999) *J. Steroid Biochem. Mol. Biol. 68*, 137−144.
9. Jensen, R. T., Lemp, G. F., and Gardner, J. D. (1982) *J. Biol. Chem. 257*, 5554−5559.
10. Brand, S. J., Andersen, B. N., and Rehfeld, J. F. (1984) *Nature 309*, 456−458.
11. Roth, J. R., and Rivett, A. J. (1982) *Biochem. Pharmacol. 31*, 3017−3021.
12. Ishihara, M., Guo, Y., and Swiedler, S. J. (1993) *Glycobiology 3*, 83−88.
13. Hemmerich, S., Bertozzi, C. R., Leffler, H., and Rosen, S. D. (1994) *Biochemistry 33*, 4820−4829.
14. Robbins, P., and Lipmann, F. (1956) *J. Am. Chem. Soc. 78*, 6409−6410.
15. Robbins, P. W., and Lipman, F. (1958) *J. Biol. Chem. 233*, 686−690.
16. Leyh, T. S. (1993) *Crit. Rev. Biochem. Mol. Biol. 28*, 515−542.
17. Frey, P. A., and Arabshahi, A. (1995) *Biochemistry 34*, 11307−11310.
18. Leyh, T. S., Taylor, J. C., and Markham, G. D. (1988) *J. Biol. Chem. 263*, 2409−2416.
19. Schwedock, J. S., Liu, C., Leyh, T. S., and Long, S. R. (1994) *J. Bacteriol. 176*, 7055−7064.
20. Liu, C., Suo, Y., and Leyh, T. S. (1994) *Biochemistry 33*, 7309−7314.
21. Leyh, T. S., and Suo, Y. (1992) *J. Biol. Chem. 267*, 542−545.
22. Leyh, T. S., Vogt, T. F., and Suo, Y. (1992) *J. Biol. Chem. 267*, 10405−10410.
23. Wei, J., and Leyh, T. S. (1998) *Biochemistry 37*, 17163−17169.
24. Wei, J., and Leyh, T. S. (1999) *Biochemistry 38*, 6311−6316.
25. Wang, R., Liu, C., and Leyh, T. S. (1995) *Biochemistry 34*, 490−495.
26. Yang, M., and Leyh, T. S. (1997) *Biochemistry 36*, 3270−3277.
27. Roberts (1977) in *Enzyme Kinetics*, pp 155−157, Cambridge University Texts, London.

28. Buchler, T., and Pfleiderer, G. (1955) *Methods Enzymol. 1*, 435−440.
29. Dixon, M., and Webb, E. C. (1979) in *Enzymes*, pp 17−18, Academic Press, New York.
30. Plowman, K. M., and Krall, A. R. (1965) *Biochemistry 4*, 2809−2814.
31. McClure, W. R. (1969) *Biochemistry 8*, 2782−2786.
32. Cleland, W. W. (1979) *Methods Enzymol. 63*, 103−138.
33. Cleland, W. W. (1979) *Methods Enzymol. 63*, 500−513.
34. Randerath, K., and Randerath, E. (1964) *J. Chromatogr. 16*, 111−125.
35. Nye, L., Colclough, J. M., Johnson, B. J., and Harrison, R. M. (1988) *Am. Biotechnol. Lab. 6*, 18−26.
36. Liu, C., Martin, E., and Leyh, T. S. (1994) *Biochemistry 33*, 2042−2047.
37. Johnson, K. A. (1986) *Methods Enzymol. 134*, 677−705.
38. Johnson, K. A. (1992) *Enzymes (3rd Ed.) 20*, 1−61.

BI992210Y